2016

Target-specific glycinergic transmission from VGluT3-expressing amacrine cells shapes suppressive contrast responses in the retina

Nai-Wen Tien
Washington University School of Medicine in St. Louis

Tahnbee Kim
Washington University School of Medicine in St. Louis

Daniel Kerschensteiner
Washington University School of Medicine in St. Louis

Cell Reports

Target-Specific Glycinergic Transmission from VGluT3-Expressing Amacrine Cells Shapes Suppressive Contrast Responses in the Retina

Graphical Abstract

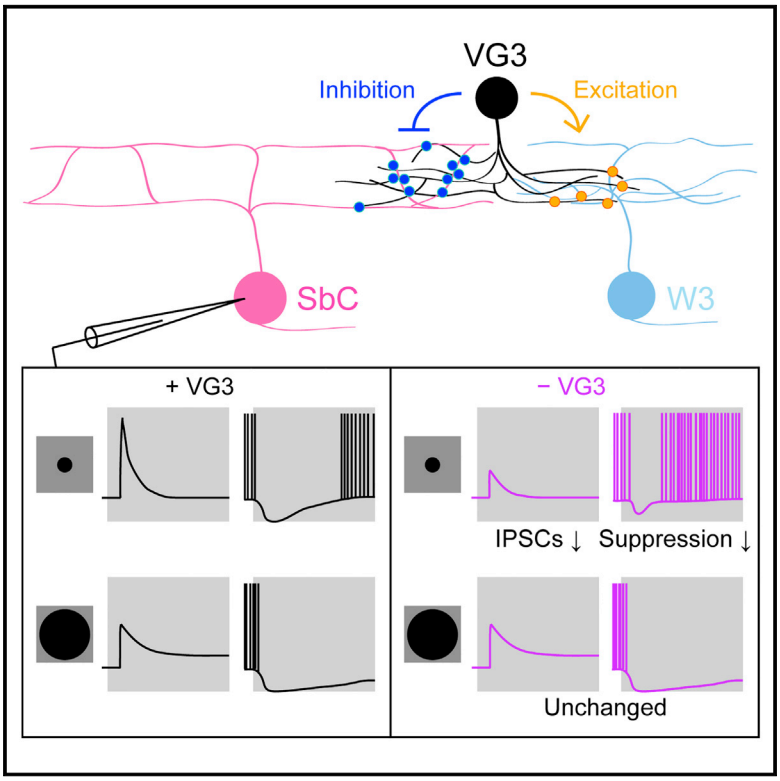

Authors

Nai-Wen Tien, Tahnbee Kim, Daniel Kerschensteiner

Correspondence

dkerschensteiner@wustl.edu

In Brief

Tien et al. show that VG3-ACs deploy dual transmitters (glycine and glutamate) in a target-specific manner and form glycinergic synapses on the link processes connecting ON and OFF arbors of SbC-RGC dendrites. Cell-type-specific deletion in mature circuits reveals contrast- and size-selective influences of VG3-ACs on SbC-RGC responses.

Highlights

- VGluT3-expressing amacrine cells (VG3-ACs) are dual transmitter neurons
- VG3-ACs provide purely glycinergic input to Suppressed-by-Contrast RGCs (SbC-RGCs)
- VG3-ACs form synapses on processes linking ON and OFF arbors of SbC-RGC dendrites
- VG3-ACs shape responses of SbC-RGCs in a contrast- and size-selective manner

Tien et al., 2016, Cell Reports *15*, 1369–1375
May 17, 2016
http://dx.doi.org/10.1016/j.celrep.2016.04.025

CellPress

Cell Reports
Report

Target-Specific Glycinergic Transmission from VGluT3-Expressing Amacrine Cells Shapes Suppressive Contrast Responses in the Retina

Nai-Wen Tien,[1,2] Tahnbee Kim,[1,2] and Daniel Kerschensteiner[1,3,4,5,*]
[1]Department of Ophthalmology and Visual Sciences
[2]Graduate Program in Neuroscience
[3]Department of Neuroscience
[4]Department of Biomedical Engineering
[5]Hope Center for Neurological Disorders
Washington University School of Medicine, Saint Louis, MO 63110, USA
*Correspondence: dkerschensteiner@wustl.edu
http://dx.doi.org/10.1016/j.celrep.2016.04.025

SUMMARY

Neurons that release more than one transmitter exist throughout the CNS. Yet, how these neurons deploy multiple transmitters and shape the function of specific circuits is not well understood. VGluT3-expressing amacrine cells (VG3-ACs) provide glutamatergic input to ganglion cells activated by contrast and motion. Using optogenetics, we find that VG3-ACs provide selective glycinergic input to a retinal ganglion cell type suppressed by contrast and motion (SbC-RGCs). Firing of SbC-RGCs is suppressed at light ON and OFF over a broad range of stimulus sizes. Anatomical circuit reconstructions reveal that VG3-ACs form inhibitory synapses preferentially on processes that link ON and OFF arbors of SbC-RGC dendrites. Removal of VG3-ACs from mature circuits reduces inhibition and attenuates spike suppression of SbC-RGCs in a contrast- and size-selective manner, illustrating the modularity of retinal circuits. VG3-ACs thus use dual transmitters in a target-specific manner and shape suppressive contrast responses in the retina by glycinergic transmission.

INTRODUCTION

Classically, each neuron was thought to use a single transmitter to send uniform signals across all its synapses (i.e., Dale's principle) (Strata and Harvey, 1999). In recent years, however, it has become clear that the output of neurons can be more diverse (Hnasko and Edwards, 2012; Vaaga et al., 2014). Neurons that release neuromodulatory peptides or monoamines often release a fast transmitter as well, emitting parallel signals that act over different spatial and temporal scales (Contini and Raviola, 2003; Nusbaum et al., 2001; Tritsch et al., 2012). In addition, some neurons release two fast transmitters. The identification of dual-transmitter neurons has been facilitated by optogenetics, and co-release of excitatory (Gras et al., 2008; Ren et al., 2011), inhibitory (Apostolides and Trussell, 2013; Jonas et al., 1998; Wojcik et al., 2006), and excitatory and inhibitory fast transmitters (Noh et al., 2010; O'Malley et al., 1992; Root et al., 2014; Saunders et al., 2015) have all been reported. How neurons use dual transmitters to support specific circuit functions, however, is not well understood.

Some dual transmitters share a vesicular transporter (Jonas et al., 1998; Tritsch et al., 2012; Wojcik et al., 2006) or are packaged into the same vesicles by synergistic action of two transporters (Gras et al., 2008; Hnasko and Edwards, 2012). These transmitters are co-released at all synapses of the respective neurons, which send the same complex signal to all their targets. By contrast, recent studies revealed spatial separation of vesicle pools containing monoamines and fast neurotransmitters in some axons (Chuhma et al., 2014; Gagnon and Parent, 2014; Onoa et al., 2010; Zhang et al., 2015). This in principle enables the respective neurons to send different messages to different targets. Whether neurons can selectively deploy two fast transmitters, particularly excitatory and inhibitory ones, to send opposite signals to specific targets and, if so, how these signals shape the function of postsynaptic partners are unclear.

Amacrine cells (ACs) are a diverse class of retinal interneurons. One of the 30–50 distinct AC types in mice expresses the vesicular glutamate transporter 3 (VGluT3). VGluT3-expressing ACs (VG3-ACs) are conserved from rodents to primates (Haverkamp and Wässle, 2004; Johnson et al., 2004) and prefer light decrements (OFF) to increments (ON) (Grimes et al., 2011; Kim et al., 2015; Lee et al., 2014) and small stimuli to large ones (i.e., size selectivity) (Kim et al., 2015; Lee et al., 2014). Recent anatomic and functional studies showed that VG3-ACs provide selective glutamatergic input to several types of retinal ganglion cells (RGCs), output neurons of the eye, which share response properties with VG3-ACs (Kim et al., 2015; Krishnaswamy et al., 2015; Lee et al., 2014). Elsewhere in the nervous system, VGluT3 is associated with dual transmitter phenotypes (Gagnon and Parent, 2014; Gras et al., 2008; Noh et al., 2010). VG3-ACs express an uptake transporter for glycine and accumulate glycine in their cytosol but appear to lack the transporter for its vesicular packaging (Haverkamp and Wässle, 2004; Johnson et al., 2004). Thus, whether VG3-ACs release glycine, which RGC types are

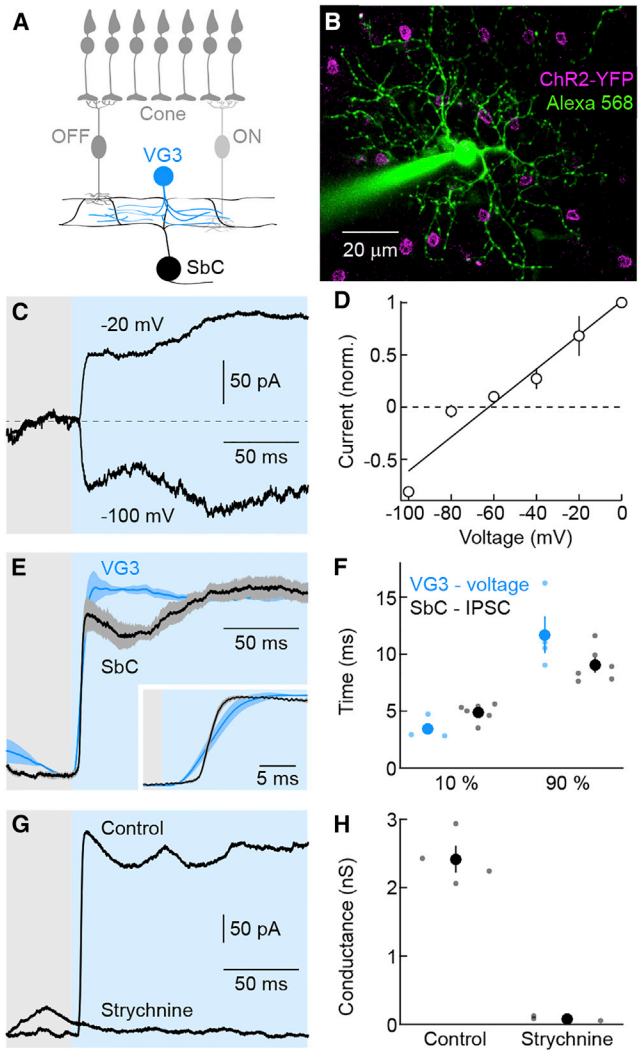

Figure 1. VG3-ACs Provide Direct Glycinergic Input to SbC-RGCs

(A) Schematic of the retina. Cone photoreceptors distribute signals to ON and OFF bipolar cells, which converge onto VG3-ACs. Neurites of VG3-ACs overlap with link processes between ON and OFF arbors of SbC-RGC dendrites.

(B) Representative SbC-RGC recorded in a *VG3-ChR2* retina. The image is a z axis projection of a two-photon image stack. Whereas the Alexa 568 signal (green) was projected through the complete stack, projection of the YFP fluorescence (magenta) was restricted to the inner nuclear layer to highlight somata of VG3-ACs.

(C and D) Representative traces (C) and summary data (D, mean ± SEM, n = 5) of currents recorded at different holding potentials in SbC-RGCs during optogenetic stimulation of VG3-ACs.

(E) VG3-AC voltage (blue) and SbC-RGCs IPSC (black) responses to a bright step of blue light (3.15×10^{-4} W mm^{-2}, 426–446 nm, shaded area). Lines (shaded areas) indicate normalized mean (±SEM) responses, facilitating comparisons of response timing. The inset shows responses at the stimulus onset on an expanded timescale.

(F) Summary data of the time after stimulus onset before 10% and 90% of the peak amplitudes are reached (VG3-AC voltage, blue; SbC-RGC IPSC, black). Dots show data from individual cells (VG3-AC voltage, n = 4; SbC-RGC IPSC, n = 6) and circles (error bars) indicate mean (±SEM) of the respective population ($p < 0.03$ for 10%; $p > 0.1$ for 90%).

(G and H) Representative IPSC traces (G) and summary data of inhibitory conductances (H) of SbC-RGC elicited by optogenetic stimulation of VG3-ACs in absence or presence of strychnine. Dots represent data from individual cells (control, n = 4; strychnine, n = 3, $p < 0.001$) and circles (error bars) indicate mean (±SEM) of the respective population.

See also Figures S1 and S2.

targets of this putative inhibitory transmission and how their output is shaped by VG3-AC input is unknown.

Unlike other RGCs, Suppressed-by-Contrast RGCs (SbC-RGCs) encode contrast through depressions in tonic firing (Levick, 1967; Rodieck, 1967). SbC-RGCs are conserved from rodents to primates (de Monasterio, 1978; Tien et al., 2015) and are suppressed by ON and OFF stimuli, both large and small (Jacoby et al., 2015; Tien et al., 2015). Their responses propagate through the retino-geniculo-cortical pathway (Niell and Stryker, 2010; Piscopo et al., 2013). The circuit mechanisms giving rise to the unique responses of SbC-RGCs are incompletely understood but involve strong inhibitory synaptic inputs at light ON and OFF (Sivyer et al., 2010; Tien et al., 2015). A recent study revealed that ON inhibition is mediated by Crh1-ACs and likely AII-ACs (Jacoby et al., 2015). The source of OFF inhibition remains unknown.

Using optogenetics, we discover that VG3-ACs provide selective glycinergic input to SbC-RGCs. Anatomic circuit reconstructions reveal that VG3-ACs form inhibitory synapses preferentially on the ascending and descending processes that link the bistratified dendrites of SbC-RGCs. Genetic deletion of VG3-ACs in mature circuits reduces OFF inhibition to SbC-RGCs particularly in response to small stimuli and attenuates suppressive spike responses with similar contrast bias and size selectivity. VG3-ACs thus are dual-transmitter neurons that deploy excitatory and inhibitory transmitters in a target-specific manner, using glycinergic transmission to shape suppressive contrast responses in the retina.

RESULTS

To identify sources of inhibitory input to SbC-RCCs, we crossed mice expressing channelrhodopsin-2 fused to yellow fluorescent protein (ChR2-YFP, *ChR2* mice) in a Cre-dependent manner (Madisen et al., 2012) to different driver lines, including *VG3-Cre* (Grimes et al., 2011). Based on two-photon guided recordings in *VG3-Cre ChR2* double transgenic mice (*VG3-ChR2* mice), we chose optogenetic stimulus parameters that match depolarizations of VG3-ACs to their photoreceptor-mediated light responses (Figure S1). Optogenetic stimulation with these parameters elicited large postsynaptic currents in all (7/7) SbC-RGCs tested. These currents reverse at –68.7 ± 4.2 mV (Figures 1A–1D), close to the expected reversal potential for chloride conductances (−60 mV) in our recording conditions, suggesting that VG3-ACs, which previously have been shown to provide excitatory input to several RGC types (Kim et al., 2015; Krishnaswamy et al., 2015; Lee et al., 2014), provide inhibitory input to SbC-RGCs. The delay of ChR2-mediated inhibitory postsynaptic currents (IPSCs) is much shorter than that of photoreceptor-mediated IPSCs (Figure S2). Indeed, ChR2-mediated IPSCs in SbC-RGCs begin to rise <2 ms after the voltage of VG3-ACs and peak before the voltage response (Figures 1E and 1F). The

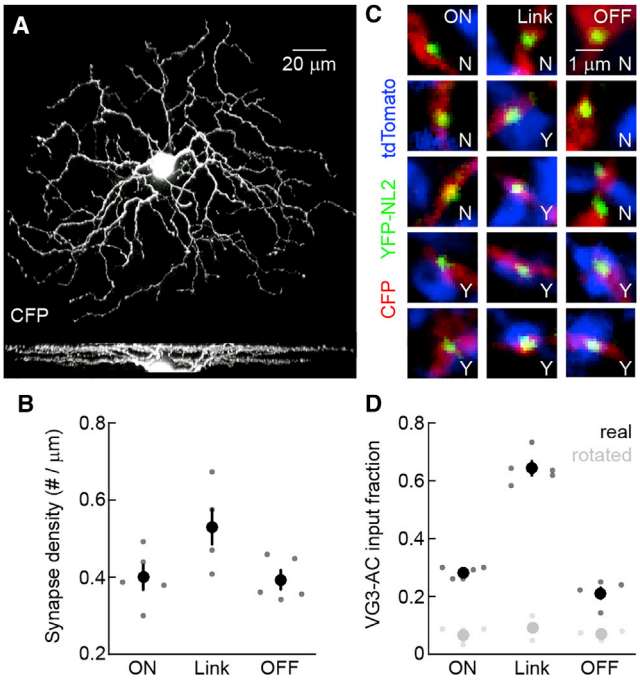

Figure 2. VG3-ACs Form Inhibitory Synapses on Link Processes of SbC-RGC Dendrites

(A) z (top) and y axis (bottom) projections of a confocal image stack of a representative CFP-expressing SbC-RGC labeled by biolistics.

(B) Summary data (n = 5) comparing inhibitory synapse density among ON dendrites, link processes, and OFF dendrites ($p < 0.05$ for ON dendrites versus link processes, $p < 0.03$ for OFF dendrites versus link processes, and $p > 0.8$ for ON versus OFF dendrites). Dots represent data from individual cells and circles (error bars) indicate mean (±SEM) of the respective populations.

(C) Excerpts of single-image planes in the ON dendrite (left column), link process (middle column), and OFF dendrite (right column) portions of a confocal image stack of an SbC-RGC. SbC-RGC dendrites are labeled with CFP (red), inhibitory postsynaptic sites with YFP-NL2 (green) and VG3-AC neurites with tdTomato (blue, *VG3-tdT* retina). The presence and absence of VG3-AC boutons at inhibitory synapses on SbC-RGC dendrites is indicated by Y and N, respectively.

(D) Summary data (n = 5) comparing the fraction of inhibitory synapses apposed by VG3-AC neurites among ON dendrites, link processes, and OFF dendrites ($p < 10^{-6}$ for ON and OFF dendrites versus link processes, $p < 0.001$ for ON versus OFF dendrites). Black dots show data from individual cells and black circles (error bars) represent mean (±SEM). For all processes (i.e., ON dendrites, link processes, and OFF dendrites), the fraction of synapses with appositions was lower ($p < 0.003$) when the VG3-AC signal was rotated by 90° (gray dots and circles), confirming the significance of this co-localization.

short delay of IPSCs and their persistence in the presence of AMPA and NMDA receptor blockers (Figure S2) rule out di-synaptic pathways driven by glutamate release from VG3-ACs as their source. ChR2-mediated IPSCs are abolished by application of strychnine (Figures 1G and 1H). Together, these results show that VG3-ACs provide direct glycinergic input to SbC-RGCs.

SbC-RGCs are bistratified neurons whose ON and OFF dendrites are linked by numerous ascending and descending processes (Sivyer and Vaney, 2010; Tien et al., 2015). To determine the sites of inhibitory input from VG3-ACs, we biolistically labeled SbC-RGCs with cyan fluorescent protein (CFP) and YFP fused to neuroligin 2 (YFP-NL2), a selective marker of inhibitory synapses on RGC dendrites (Soto et al., 2011), in mice that express tdTomato in VG3-ACs. The density of inhibitory synapses was highest on link processes between ON and OFF arbors (Figures 2A and 2B). A majority of these synapses were apposed by boutons of VG3-ACs, compared to a lower fraction of such appositions on ON and OFF dendrites (Figures 2C and 2D). Thus, VG3-ACs appear to provide glycinergic input to SbC-RGCs preferentially through synapses on link processes, both a characteristic and conserved feature of SbC-RGC dendrites.

To elucidate the contribution of VG3-ACs to inhibition of SbC-RGCs during visual processing, we selectively removed VG3-ACs from mature circuits. Toward this end, we injected *VG3-DTR* and control mice intraperitoneally with diphtheria toxin starting at postnatal day 30 (see Experimental Procedures) (Krishnaswamy et al., 2015). VGluT3 staining showed that the density of VG3-ACs was reduced by >90% 1 week after injections in *VG3-DTR* mic, but remained unchanged in littermate controls (Figures 3A and 3B) (Kim et al., 2015). The density of other amacrine cells was unaffected in *VG3-DTR* mice (Figure S3), confirming the specificity of this manipulation. Comparing IPSCs elicited by contrast steps presented in spots of different size between *VG3-DTR* and control mice, we found that OFF but not ON inhibition to SbC-RGCs was reduced in a size-selective manner by removal of VG3-ACs (Figures 3C–3F). Responses of VG3-ACs match the size selectivity of this deficit (Kim et al., 2015). VG3-ACs respond more strongly to OFF than ON stimuli (Kim et al., 2015). The preservation of ON inhibition in *VG3-DTR* mice suggests either that VG3-AC responses to ON stimuli fail to elicit glycine release or that other ON-responsive amacrine cells compensate for lost input from VG3-ACs (Jacoby et al., 2015).

To determine how inhibitory input from VG3-ACs shapes spike responses of SbC-RGCs, we obtained current-clamp recordings in *VG3-DTR* and control mice. Consistent with the reduced inhibitory input and reduced suppression of tonic excitation (Figure S4), spike suppression of SbC-RGCs by OFF stimuli was attenuated in a size-selective manner by removal of VG3-ACs (Figures 4C and 4D). By contrast, suppression by ON stimuli was enhanced (Figures 4A and 4B). Voltage-clamp recordings revealed that this enhanced suppression is a result of a decrease in the ON-signed excitatory input to SbC-RGCs (Jacoby et al., 2015; Tien et al., 2015) in *VG3-DTR* compared to control mice (Figures 4E and 4F), suggesting presynaptic actions of VG3-ACs in this circuit.

DISCUSSION

Here, we discover that VG3-ACs, which previously had been shown to provide glutamatergic input to four RGC types (Kim et al., 2015; Krishnaswamy et al., 2015; Lee et al., 2014), provide glycinergic input to SbC-RGCs (Figure 1). Concurrent with our finding, another study came to the same conclusion (Lee et al., 2016). In addition, we reconstruct circuits anatomically (Figure 2) and find that VG3-ACs form inhibitory synapses preferentially on ascending and descending processes that link the bistratified dendrites of SbC-RGCs. Finally, using cell-type-specific deletion in mature circuits, we show that VG3-ACs shape suppressive

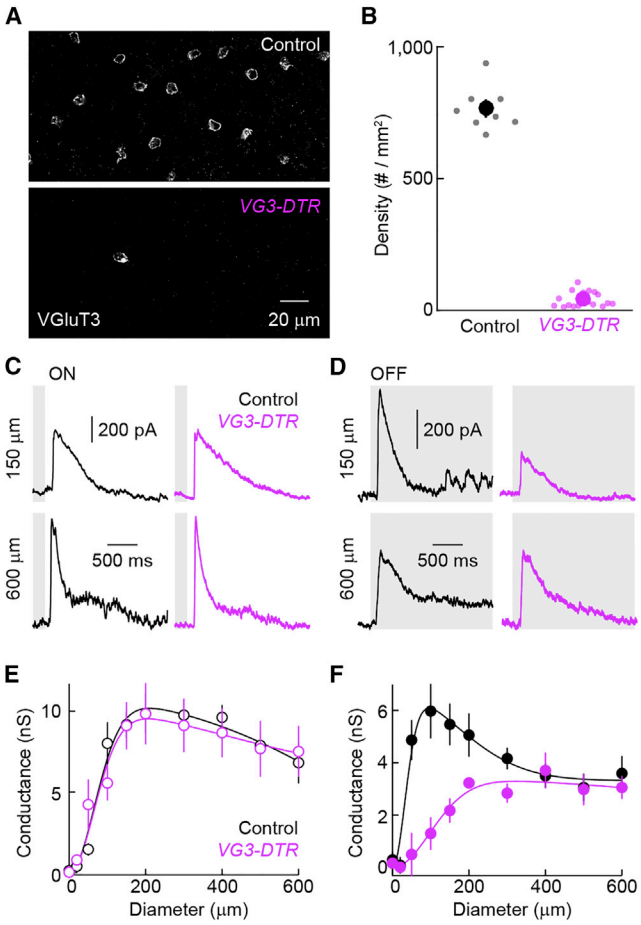

Figure 3. Genetic Removal of VG3-ACs Reduces Inhibition of SbC-RGCs in a Contrast- and Size-Selective Manner

(A) Representative z axis projections of confocal image stacks of retinal whole mounts stained for VGluT3 in control (top) and *VG3-DTR* mice (bottom) 1 week after diphtheria toxin injections.

(B) Summary data of VG3-AC density in control (black) and *VG3-DTR* (purple) retinas. Dots show data from individual retinas (control, n = 8; *VG3-DTR*, n = 18, $p < 10^{-20}$) and circles (error bars) represent mean (±SEM).

(C and D) Representative IPSCs in SbC-RGCs elicited by light increments (C, ON) and decrements (D, OFF) in small (150 μm diameter, top) or large (600 μm diameter, bottom) circles recorded in control (left, black) and *VG3-DTR* (right, purple) retinas.

(E and F) Summary plots (mean ± SEM) comparing inhibitory synaptic conductances in SbC-RGCs of control (n = 5, black) and *VG3-DTR* (n = 4, purple) retinas elicited by ON (E) and OFF (F) stimuli of different sizes (i.e., circle diameters). Inhibitory conductances elicited by small and large ON stimuli are unaffected by deletion of VG3-ACs (e.g., $p > 0.7$ for control versus *VG3-DTR* at 150 μm and 600 μm). Inhibitory conductances activated by small ($p < 0.01$ for control versus *VG3-DTR* at 150 μm) but not large ($p > 0.5$ for control versus *VG3-DTR* at 600 μm) OFF stimuli are reduced by removal of VG3-ACs.

See also Figure S3.

responses of SbC-RGCs in a contrast- and size-selective manner (Figures 3 and 4).

What mechanisms underlie the target specificity of excitatory and inhibitory neurotransmission from VG3-ACs? Glutamate and glycine could be co-released at the same synapses with specificity arising from postsynaptic receptor expression and/or localization, or they could be released selectively at synapses with different targets. In striatum, glutamate and acetylcholine are packaged into the same vesicles by synergistic action of VGluT3 and the vesicular acetylcholine transporter (VAChT) (Gras et al., 2008); GABA and glycine share a vesicular transporter (VIAAT) and are co-released in the spinal cord (Jonas et al., 1998; Wojcik et al., 2006); and GABA was recently shown to use the vesicular monoamine transporter (VMAT) to co-release with dopamine in striatum (Tritsch et al., 2012). In each of these cases, both transmitters elicit signals in each postsynaptic target cell. In other neurons, including starburst amacrine cells (Lee et al., 2010; Wei et al., 2011; Yonehara et al., 2011), dual transmitters are released from separate vesicle pools, which can segregate into different axon terminals (Chuhma et al., 2014; Gagnon and Parent, 2014; Onoa et al., 2010). The distribution of VGluT3 is homogenous along VG3-AC neurites, and VIAAT, the vesicular transporter for glycine, appears not to be expressed by VG3-ACs (Haverkamp and Wässle, 2004; Johnson et al., 2004). Whether the selectivity of excitatory and inhibitory neurotransmission between VG3-ACs and RGC targets arises pre- or postsynaptic, and whether release of glycine involves mechanisms other than vesicle fusion (Rosenberg et al., 2013), thus remains to be determined.

The observation that VG3-ACs use glutamate to excite neurons activated by contrast and motion and glycine to inhibit neurons suppressed by contrast and motion illustrates how modular output signals can enhance the circuit function of a neuron. Similar modular organization is found in the input to SbC-RGCs. Inhibition from Crh1-ACs, AII-ACs, and VG3-ACs and at least one more OFF-responsive amacrine cell combines to suppress tonic firing of SbC-RGCs (Figures 3 and 4) (Jacoby et al., 2015; Tien et al., 2015). Each convergent input contributes a distinct component of inhibition based on its preferential responses to ON or OFF, and small or large stimuli. Convergence modularity is also a feature of inhibitory input to direction selective ganglion cells (Hoggarth et al., 2015) and may be a general organizing principle of inhibitory circuits in the retina.

The numerous ascending and descending processes between ON and OFF dendrites are a characteristic feature of SbC-RGCs (Sivyer and Vaney, 2010; Tien et al., 2015). Here, we find that these link processes are the primary site of synaptic input from VG3-ACs (Figure 2), whose neurites stratify between ON and OFF arbors of SbC-RGCs. SbC-RGC link processes and the lamination of VG3-ACs are conserved from rodents to primates (Haverkamp and Wässle, 2004; Sivyer and Vaney, 2010; Tien et al., 2015), suggesting that their connectivity patterns are as well. In this unusual anatomical arrangement, VG3-ACs use their inhibitory transmitter in a target-specific manner to shape suppressive contrast responses of SbC-RGCs.

EXPERIMENTAL PROCEDURES

Mice

We used BAC transgenic mice in which Cre recombinase is expressed under control of regulatory sequences of the *Slc17a8* gene, which encodes VGluT3 (*VG3-Cre* mice), to genetically target VG3-ACs (Grimes et al., 2011; Kim et al., 2015). Ai32 and Ai9 mice, which express channelrhodopsin-2 fused to yellow fluorescent protein (ChR2-YFP) and tdTomato in a Cre-dependent manner (Madisen et al., 2012; Madisen et al., 2010) were crossed to *VG3-Cre*

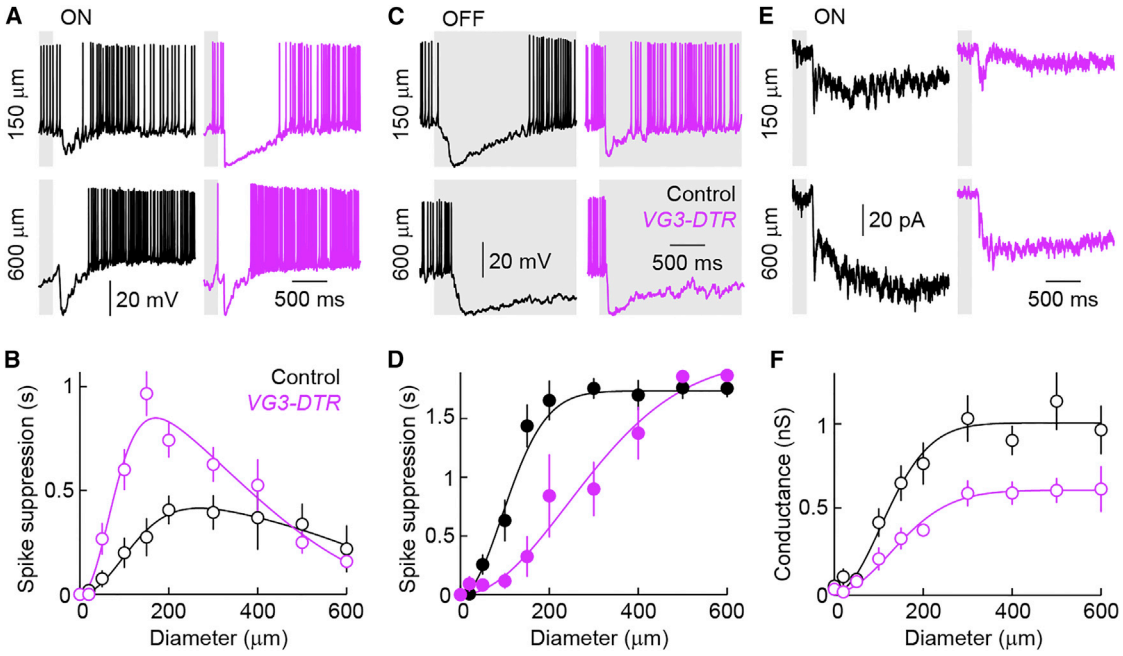

Figure 4. Genetic Removal of VG3-ACs Alters Spike Suppression and Excitatory Input of SbC-RGCs in a Contrast- and Size-Selective Manner

(A and C) Representative spike responses of SbC-RGCs to light increments (A, ON) and decrements (C, OFF) in small (150 µm diameter, top) and large (600 µm diameter, bottom) circles recorded in control (left, black) and *VG3-DTR* (right, purple) retinas.

(B and D) Summary plots (mean ± SEM) comparing the duration of spike suppression of SbC-RGCs of control (n = 8, black) and *VG3-DTR* (n = 6, purple) retinas elicited by ON (B) and OFF (D) stimuli of different sizes. Spike suppression by small ON stimuli is enhanced ($p < 0.001$ for control versus *VG3-DTR* at 150 µm) and spike suppression small OFF stimuli is reduced ($p < 0.001$ for control versus *VG3-DTR* at 150 µm) by removal of VG3-ACs. By contrast, responses to large ON and OFF stimuli are unchanged ($p > 0.6$ and $p > 0.2$ for control versus *VG3-DTR* for 600 µm ON and OFF stimuli, respectively).

(E) Representative excitatory postsynaptic current traces elicited by small (150 µm diameter, top) and large (600 µm diameter, bottom) ON stimuli.

(F) Summary data of excitatory conductances of SbC-RGCs in control (n = 7, black) and *VG3-DTR* (n = 7, purple) retinas activated by ON stimuli of different sizes. Excitatory input is reduced significantly for small ON stimuli ($p < 0.02$ for control versus *VG3-DTR* at 150 µm).

See also Figure S4.

mice for optogenetic stimulation (*VG3-ChR2* mice) and VG3-AC visualization in anatomical experiments (*VG3-tdT* mice), respectively. Mice in which the diphtheria toxin receptor (DTR) is expressed upon Cre-mediated recombination (Buch et al., 2005) were used to remove VG3-ACs after circuit development (*VG3-DTR* mice). Diphtheria toxin (1 µg/50 g body weight) was injected intraperitoneally in *VG3-DTR* mice and Cre-negative or DTR-negative littermate controls (i.e., control mice), once a day every other day for a total of four injections starting at postnatal day 30. Mice were used approximately 1 week after the last injection. All procedures in this study were approved by the Animal Studies Committee of Washington University School of Medicine and performed in compliance with the NIH Guide for the Care and Use of Laboratory Animals.

Electrophysiology

Patch-clamp recordings of SbC-RGCs were obtained in retinal flat-mount preparations. SbC-RGCs were identified based on contrast responses in loose-patch recordings, labeled by inclusion of Alexa 568 (1 mM) in the intracellular solution in subsequent whole-cell recordings and visualized by two-photon imaging at the end of each recording. During recordings, tissue was continually perfused (~8 ml/min) with warm (~33°C) mouse artificial cerebrospinal fluid ($mACSF_{NaHCO3}$) containing (in mM) 125 NaCl, 2.5 KCl, 1 $MgCl_2$, 1.25 NaH_2PO_4, 2 $CaCl_2$, 20 glucose, 26 $NaHCO_3$, and 0.5 L-glutamine equilibrated with 95% O_2/ 5% CO_2. In optogenetic experiments, L-AP4 (20 µM) and ACET (10 µM) were included in the $mACSF_{NaHCO3}$ to block transmission of photoreceptor signals to ON and OFF bipolar cells, respectively. Strychnine (1 µM) was added to $mACSF_{NaHCO3}$ to block glycinergic transmission. Current-clamp recordings were performed with an intracellular solution containing (in mM) 125 K-gluconate, 10 NaCl, 1 $MgCl_2$, 10 EGTA, 5 HEPES, 5 ATP-Na2, and 0.1 GTP-Na (pH adjusted to 7.2 with KOH). The intracellular solution used in voltage-clamp recordings contained (in mM) 120 Cs-gluconate, 1 $CaCl_2$, 1 $MgCl_2$, 10 Na-HEPES, 11 EGTA, 10 TEA-Cl, 2 Qx314, ATP-Na2, and 0.1 GTP-Na (pH adjusted to 7.2 with CsOH). Patch pipettes had resistances of 4–7 MΩ (borosilicate glass). All reported voltages were corrected for liquid junction potentials. For voltage-clamp recordings, series resistance (10–15 MΩ) was compensated electronically by ~75%. Signals were amplified with a Multiclamp 700B amplifier (Molecular Devices), filtered at 3 kHz (eight-pole Bessel low-pass), and sampled at 10 kHz (Digidata 1440A, Molecular Devices). Inhibitory and excitatory synaptic inputs to SbC-RGCs during photoreceptor-mediated light responses were isolated by holding cells at the reversal potential of excitatory (0 mV) and inhibitory (−60 mV) conductances, respectively. In current-clamp recordings, no bias current was injected.

Light Stimulation

To activate ChR2, light stimuli were presented through a 20 × 0.95 numerical aperture (NA) water immersion objective on the RGC side of the retina. Light from a mercury bulb (Olympus) was band-pass filtered (426–446 nm, Chroma) and attenuated by neutral density filters (Chroma). We performed targeted recordings from VG3-ACs to choose an optogenetic stimulus intensity (3.15×10^{-4} W mm^{-2}; Figure S1) that matches photoreceptor-mediated light responses (Kim et al., 2015). Stimulus timing was controlled by a Uniblitz shutter (Vincent Associates).

To characterize photoreceptor-mediated responses, light stimuli were presented on an organic light-emitting display (eMagin) focused on the photoreceptor side of the retina via the substage condenser. Intensity of spots of

varying size was square-wave-modulated at 0.25 Hz (average intensity: 1,500 rhodopsin isomerizations rod^{-1} s^{-1}; Michelson contrast: 100%). The order in which spots of different size were presented was randomly chosen for each cell. IPSC amplitudes were measured as baseline subtracted averages during 200-ms time windows. The duration of spike suppression was defined as the time following a stimulus during which the firing rate was below 50% of the average firing rate (Jacoby et al., 2015).

Biolistics and Imaging

Gold particles (1.6 μm diameter, Bio-Rad) were coated with plasmids encoding cytosolic CFP and neuroligin 2 fused at its N terminus to yellow fluorescent protein (YFP-NL2). Particles were delivered to RGCs from a helium-pressurized gun (Bio-Rad) at approximately 40 psi (Kim et al., 2015). After shooting, retinal flat-mount preparations in $ACSF_{HEPES}$, containing (in mM) 119 NaCl, 2.5 KCl, 2.5 $CaCl_2$, 1.3 $MgCl_2$, 1 NaH_2PO_4, 11 glucose, and 20 HEPES (pH adjusted to 7.37 with NaOH), were incubated in a humid oxygenated chamber at 33–35°C for 14–18 hr. The tissue was then fixed for 30 min in 4% paraformaldehyde in $mACSF_{HEPES}$ and washed PBS (3 × 10 min) before mounting and imaging. Confocal image stacks of biolistically labeled SbC-RGCs in *VG3-tdT* mice were acquired on Fv1000 laser scanning microscopes (Olympus) using a 60× 1.35 NA oil immersion objective. Synaptic connectivity was analyzed in image stacks with voxel size 0.103 μm (x/y axis) – 0.3 μm (z axis). Using local thresholding SbC-RGC dendrites, YFP-NL2 puncta and VG3-AC neurites were masked separately in Amira (FEI Company). Inhibitory synapses on SbC-RGCs formed by VG3-ACs were defined as YFP-NL2 clusters with a center of mass within 0.5 μm from a VG3-AC neurite. We confirmed that varying this distance from 0.25 to 1 μm did not qualitatively change the results. Given the size of synaptic puncta, this range implies overlap or direct apposition of signals from YFP-NL2 and tdTomato in VG3-AC neurites. To compare the fraction of YFP-NL2 apposed by VG3-AC neurites to that caused by random signal overlap, the same analysis was repeated for each cell in image stacks in which the VG3-AC channel was rotated by 90° (i.e., switching x and y axes).

Statistics

Paired and unpaired t tests were used to assess the statistical significance of observed differences.

SUPPLEMENTAL INFORMATION

Supplemental Information includes four figures and can be found with this article online at http://dx.doi.org/10.1016/j.celrep.2016.04.025.

AUTHOR CONTRIBUTIONS

N.-W.T., T.K., and D.K. designed, performed, and analyzed experiments and wrote the manuscript.

ACKNOWLEDGMENTS

We thank members of D.K.'s lab for helpful discussion and comments on the manuscript. We are grateful to Dr. Robert Edwards for sharing *VG3-Cre* mice with us. This work was supported by the Research to Prevent Blindness Foundation (Career Development Award to D.K. and an unrestricted grant to the Department of Ophthalmology and Visual Sciences at Washington University) and the NIH (EY021855 and EY023341 to D.K. and EY0268 to the Department of Ophthalmology and Visual Sciences at Washington University).

Received: March 10, 2016
Revised: March 28, 2016
Accepted: April 3, 2016
Published: May 5, 2016

REFERENCES

Apostolides, P.F., and Trussell, L.O. (2013). Rapid, activity-independent turnover of vesicular transmitter content at a mixed glycine/GABA synapse. J. Neurosci. *33*, 4768–4781.

Buch, T., Heppner, F.L., Tertilt, C., Heinen, T.J., Kremer, M., Wunderlich, F.T., Jung, S., and Waisman, A. (2005). A Cre-inducible diphtheria toxin receptor mediates cell lineage ablation after toxin administration. Nat. Methods *2*, 419–426.

Chuhma, N., Mingote, S., Moore, H., and Rayport, S. (2014). Dopamine neurons control striatal cholinergic neurons via regionally heterogeneous dopamine and glutamate signaling. Neuron *81*, 901–912.

Contini, M., and Raviola, E. (2003). GABAergic synapses made by a retinal dopaminergic neuron. Proc. Natl. Acad. Sci. USA *100*, 1358–1363.

de Monasterio, F.M. (1978). Properties of ganglion cells with atypical receptive-field organization in retina of macaques. J. Neurophysiol. *41*, 1435–1449.

Gagnon, D., and Parent, M. (2014). Distribution of VGLUT3 in highly collateralized axons from the rat dorsal raphe nucleus as revealed by single-neuron reconstructions. PLoS ONE *9*, e87709.

Gras, C., Amilhon, B., Lepicard, E.M., Poirel, O., Vinatier, J., Herbin, M., Dumas, S., Tzavara, E.T., Wade, M.R., Nomikos, G.G., et al. (2008). The vesicular glutamate transporter VGLUT3 synergizes striatal acetylcholine tone. Nat. Neurosci. *11*, 292–300.

Grimes, W.N., Seal, R.P., Oesch, N., Edwards, R.H., and Diamond, J.S. (2011). Genetic targeting and physiological features of VGLUT3+ amacrine cells. Vis. Neurosci. *28*, 381–392.

Haverkamp, S., and Wässle, H. (2004). Characterization of an amacrine cell type of the mammalian retina immunoreactive for vesicular glutamate transporter 3. J. Comp. Neurol. *468*, 251–263.

Hnasko, T.S., and Edwards, R.H. (2012). Neurotransmitter corelease: mechanism and physiological role. Annu. Rev. Physiol. *74*, 225–243.

Hoggarth, A., McLaughlin, A.J., Ronellenfitch, K., Trenholm, S., Vasandani, R., Sethuramanujam, S., Schwab, D., Briggman, K.L., and Awatramani, G.B. (2015). Specific wiring of distinct amacrine cells in the directionally selective retinal circuit permits independent coding of direction and size. Neuron *86*, 276–291.

Jacoby, J., Zhu, Y., DeVries, S.H., and Schwartz, G.W. (2015). An Amacrine Cell Circuit for Signaling Steady Illumination in the Retina. Cell Rep. *13*, 2663–2670.

Johnson, J., Sherry, D.M., Liu, X., Fremeau, R.T., Jr., Seal, R.P., Edwards, R.H., and Copenhagen, D.R. (2004). Vesicular glutamate transporter 3 expression identifies glutamatergic amacrine cells in the rodent retina. J. Comp. Neurol. *477*, 386–398.

Jonas, P., Bischofberger, J., and Sandkühler, J. (1998). Corelease of two fast neurotransmitters at a central synapse. Science *281*, 419–424.

Kim, T., Soto, F., and Kerschensteiner, D. (2015). An excitatory amacrine cell detects object motion and provides feature-selective input to ganglion cells in the mouse retina. eLife *4*, 4.

Krishnaswamy, A., Yamagata, M., Duan, X., Hong, Y.K., and Sanes, J.R. (2015). Sidekick 2 directs formation of a retinal circuit that detects differential motion. Nature *524*, 466–470.

Lee, S., Kim, K., and Zhou, Z.J. (2010). Role of ACh-GABA cotransmission in detecting image motion and motion direction. Neuron *68*, 1159–1172.

Lee, S., Chen, L., Chen, M., Ye, M., Seal, R.P., and Zhou, Z.J. (2014). An unconventional glutamatergic circuit in the retina formed by vGluT3 amacrine cells. Neuron *84*, 708–715.

Lee, S., Zhang, Y., Chen, M., and Zhou, Z.J. (2016). Segregated glycine-glutamate co-transmission from vGluT3 amacrine cells to contrast-suppressed and contrast-enhanced retinal circuits. Neuron *90*, 27–34.

Levick, W.R. (1967). Receptive fields and trigger features of ganglion cells in the visual streak of the rabbits retina. J. Physiol. *188*, 285–307.

Madisen, L., Zwingman, T.A., Sunkin, S.M., Oh, S.W., Zariwala, H.A., Gu, H., Ng, L.L., Palmiter, R.D., Hawrylycz, M.J., Jones, A.R., et al. (2010). A robust and high-throughput Cre reporting and characterization system for the whole mouse brain. Nat. Neurosci. *13*, 133–140.

Madisen, L., Mao, T., Koch, H., Zhuo, J.M., Berenyi, A., Fujisawa, S., Hsu, Y.W., Garcia, A.J., 3rd, Gu, X., Zanella, S., et al. (2012). A toolbox of Cre-dependent

optogenetic transgenic mice for light-induced activation and silencing. Nat. Neurosci. *15*, 793–802.

Niell, C.M., and Stryker, M.P. (2010). Modulation of visual responses by behavioral state in mouse visual cortex. Neuron *65*, 472–479.

Noh, J., Seal, R.P., Garver, J.A., Edwards, R.H., and Kandler, K. (2010). Glutamate co-release at GABA/glycinergic synapses is crucial for the refinement of an inhibitory map. Nat. Neurosci. *13*, 232–238.

Nusbaum, M.P., Blitz, D.M., Swensen, A.M., Wood, D., and Marder, E. (2001). The roles of co-transmission in neural network modulation. Trends Neurosci. *24*, 146–154.

O'Malley, D.M., Sandell, J.H., and Masland, R.H. (1992). Co-release of acetylcholine and GABA by the starburst amacrine cells. J. Neurosci. *12*, 1394–1408.

Onoa, B., Li, H., Gagnon-Bartsch, J.A., Elias, L.A., and Edwards, R.H. (2010). Vesicular monoamine and glutamate transporters select distinct synaptic vesicle recycling pathways. J. Neurosci. *30*, 7917–7927.

Piscopo, D.M., El-Danaf, R.N., Huberman, A.D., and Niell, C.M. (2013). Diverse visual features encoded in mouse lateral geniculate nucleus. J. Neurosci. *33*, 4642–4656.

Ren, J., Qin, C., Hu, F., Tan, J., Qiu, L., Zhao, S., Feng, G., and Luo, M. (2011). Habenula "cholinergic" neurons co-release glutamate and acetylcholine and activate postsynaptic neurons via distinct transmission modes. Neuron *69*, 445–452.

Rodieck, R.W. (1967). Receptive fields in the cat retina: a new type. Science *157*, 90–92.

Root, D.H., Mejias-Aponte, C.A., Zhang, S., Wang, H.L., Hoffman, A.F., Lupica, C.R., and Morales, M. (2014). Single rodent mesohabenular axons release glutamate and GABA. Nat. Neurosci. *17*, 1543–1551.

Rosenberg, D., Artoul, S., Segal, A.C., Kolodney, G., Radzishevsky, I., Dikopoltsev, E., Foltyn, V.N., Inoue, R., Mori, H., Billard, J.M., and Wolosker, H. (2013). Neuronal D-serine and glycine release via the Asc-1 transporter regulates NMDA receptor-dependent synaptic activity. J. Neurosci. *33*, 3533–3544.

Saunders, A., Granger, A.J., and Sabatini, B.L. (2015). Corelease of acetylcholine and GABA from cholinergic forebrain neurons. eLife, Published online February 27, 2015. http://dx.doi.org/10.7554/eLife.06412.

Sivyer, B., and Vaney, D.I. (2010). Dendritic morphology and tracer-coupling pattern of physiologically identified transient uniformity detector ganglion cells in rabbit retina. Vis. Neurosci. *27*, 159–170.

Sivyer, B., Taylor, W.R., and Vaney, D.I. (2010). Uniformity detector retinal ganglion cells fire complex spikes and receive only light-evoked inhibition. Proc. Natl. Acad. Sci. USA *107*, 5628–5633.

Soto, F., Bleckert, A., Lewis, R., Kang, Y., Kerschensteiner, D., Craig, A.M., and Wong, R.O. (2011). Coordinated increase in inhibitory and excitatory synapses onto retinal ganglion cells during development. Neural Dev. *6*, 31.

Strata, P., and Harvey, R. (1999). Dale's principle. Brain Res. Bull. *50*, 349–350.

Tien, N.W., Pearson, J.T., Heller, C.R., Demas, J., and Kerschensteiner, D. (2015). Genetically identified suppressed-by-contrast retinal ganglion cells reliably signal self-generated visual stimuli. J. Neurosci. *35*, 10815–10820.

Tritsch, N.X., Ding, J.B., and Sabatini, B.L. (2012). Dopaminergic neurons inhibit striatal output through non-canonical release of GABA. Nature *490*, 262–266.

Vaaga, C.E., Borisovska, M., and Westbrook, G.L. (2014). Dual-transmitter neurons: functional implications of co-release and co-transmission. Curr. Opin. Neurobiol. *29*, 25–32.

Wei, W., Hamby, A.M., Zhou, K., and Feller, M.B. (2011). Development of asymmetric inhibition underlying direction selectivity in the retina. Nature *469*, 402–406.

Wojcik, S.M., Katsurabayashi, S., Guillemin, I., Friauf, E., Rosenmund, C., Brose, N., and Rhee, J.S. (2006). A shared vesicular carrier allows synaptic corelease of GABA and glycine. Neuron *50*, 575–587.

Yonehara, K., Balint, K., Noda, M., Nagel, G., Bamberg, E., and Roska, B. (2011). Spatially asymmetric reorganization of inhibition establishes a motion-sensitive circuit. Nature *469*, 407–410.

Zhang, S., Qi, J., Li, X., Wang, H.L., Britt, J.P., Hoffman, A.F., Bonci, A., Lupica, C.R., and Morales, M. (2015). Dopaminergic and glutamatergic microdomains in a subset of rodent mesoaccumbens axons. Nat. Neurosci. *18*, 386–392.